UV/Vis Spectra of Subporphyrazines and Subphthalocyanines with Aluminum and Gallium: A Time-Dependent DFT Study

ARTICLE *in* CHEMPHYSCHEM · APRIL 2013

Impact Factor: 3.42 · DOI: 10.1002/cphc.201201028 · Source: PubMed

4 AUTHORS:

M. Merced Montero-Campillo
Universidad Autónoma de Madrid
29 PUBLICATIONS **148** CITATIONS
SEE PROFILE

Al Mokhtar Lamsabhi
Universidad Autónoma de Madrid
70 PUBLICATIONS **805** CITATIONS
SEE PROFILE

Otilia Mó
Universidad Autónoma de Madrid
404 PUBLICATIONS **6,379** CITATIONS
SEE PROFILE

Manuel Yanez
Universidad Autónoma de Madrid
272 PUBLICATIONS **3,747** CITATIONS
SEE PROFILE

ChemPubSoc Europe

DOI: 10.1002/cphc.201201028

UV/Vis Spectra of Subporphyrazines and Subphthalocyanines with Aluminum and Gallium: A Time-Dependent DFT Study

M. Merced Montero-Campillo,* Al Mokhtar Lamsabhi, Otilia Mó, and Manuel Yáñez[a]

Dedicated to the memory of Christian Claessens

The UV/Vis spectra of selected substituted subporphyrazines (SubPz) and subphthalocyanines (SubPc) with aluminum and gallium as central atoms are analyzed through time-dependent DFT calculations in chloroform. The results are compared with previous results with boron as the central atom to analyze the photochemical properties of these two families of compounds on varying the metal along the same group. The absorptions of SubPz (Al, Ga) are redshifted or blueshifted with respect to SubPz (B) depending on the nature of the R substituents of the molecule, whereas the absorptions of SubPc (Al, Ga) structures are redshifted and with smaller energy gaps with respect to SubPc (B) for all kinds of R substituents. Looking at their absorption spectra, these systems with aluminum and gallium may also have, as in the case of boron, promising photochemical properties.

1. Introduction

During the last few decades the demand for energy in the world has increased up to its historical maximum, which has motivated the scientific community to look for alternative, cheaper, and renewable energy sources. Solar energy plays a main role in this scenario and new organic compounds with attractive optoelectronic features have been developed to take advantage of this possibility.[1–3] Photovoltaic devices are composed of donor–acceptor building blocks, in which the donor part is a species with good conductivity properties and a certain ability to remain in an excited electronic state as a consequence of sunlight exposure.

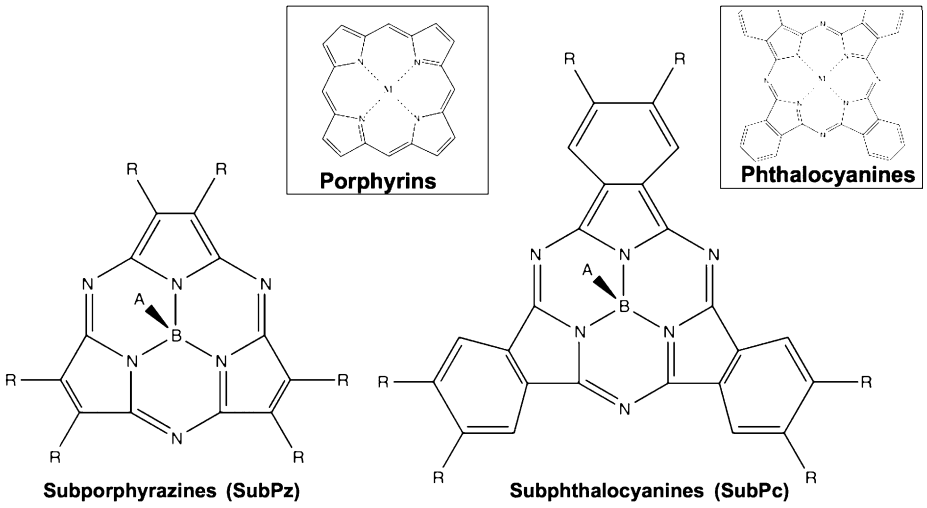

Scheme 1. Subporphyrazine (SubPz) and subphthalocyanine (SubPc) boron structures with (A, R) substituents.

Porphyrins, which are one of the most important macrocyclic ring families in organic chemistry, have derivatives and analogues with a potential optical use. Phthalocyanines (Pc), subphthalocyanines (SubPc), and subporphyrazines (SubPz) are some of them (see Scheme 1).[4,5] More than 70 metal and nonmetal ions are known to be complexed with Pc; however, as far as we know, only the boron derivatives of SubPz and SubPc have been synthesized. There is only one exception in the literature, an aluminum-SubPc complex reported in 2002.[6] Several authors have analyzed the structural differences between some of these families of compounds on varying the central ion by means of quantum mechanics calculations, including time-dependent density functional theory (TDDFT) to study their photochemical properties.[7–13]

Recently, we studied the photochemical properties of a series of substituted boron SubPz and SubPc compounds.[14] The main transitions located between 450 and 600 nm, which fall in the solar spectrum region, were predicted by using the TDDFT method. More than validating the methodology by

[a] Dr. M. M. Montero-Campillo, Prof. A. M. Lamsabhi, Prof. O. Mó, Prof. M. Yáñez
Departamento de Química, Módulo 13
Universidad Autónoma de Madrid
Campus de Excelencia UAM-CSIC
Cantoblanco, 28049 Madrid (Spain)
E-mail: mm.montero@uam.es

Supporting information for this article is available on the WWW under http://dx.doi.org/10.1002/cphc.201201028.

comparing the experimental and the theoretical UV–visible spectra, in the above-mentioned work we revealed the substituent effects (A, R) on the band shifting, thus indicating the possibility that these compounds would be good candidates for optical uses. The substitution of boron as central atom in SubPz and SubPc by atoms from the same column of the periodic table, such as aluminum or gallium, could bring changes in the photochemical behavior of these compounds. Herein, the main aim is to highlight these variations by using the same theoretical approach for selected sets of aluminum and gallium SubPz and SubPc species. After giving the technical details the main results are given, followed by discussion of some structural aspects of both SubPz and SubPc sets of molecules, and then analysis of their predicted spectra.

Computational Details

All electronic structure calculations were carried out with the B3LYP functional and 6-31G(d) basis set for all atoms with the Gaussian 09 code.[15] For each stationary point, harmonic frequencies were computed at the fully optimized geometries, which allowed the assignment of the structures as minima and the determination of zero-point energies and thermal contributions. B3LYP is a density functional theory (DFT) method that combines the three-coefficient-dependent hybrid functional for the exchange energy proposed by Becke (B3) with the correlation functional proposed by Lee, Yang, and Parr (LYP).[16]

Absorption spectra were computed considering the vertical excitations from the ground state by using time-dependent density functional linear response theory (TDDFT).[17] TDDFT is an excellent alternative for large polyatomic systems with respect to other more expensive methods (SAC-CI, STEOM-CC, or CASPT2). These calculations were carried out as single-point calculations with the same B3LYP functional and a larger Pople basis set, 6-31 + G(d,p), which includes diffuse functions on the heavy atoms. Solvent effects were evaluated by means of the polarizable continuum model (PCM) of Tomasi and co-workers using chloroform as solvent, as in previous work ($\varepsilon = 4.7113$), which has been proved to give the best results on comparison with the experimental data.[18]

The electronic spectra were simulated by means of the SWizard program package.[19] This program calculates the absorption profile as a sum of Gaussian functions using the formula [Eq. (1)]:

$$\varepsilon(\omega) = 2.174 \times 10^8 \sum_i \frac{f_i}{\Delta_{1/2}} \exp\left(-2.773 \frac{(\omega - \omega_i)^2}{\Delta_{1/2}^2}\right) \quad (1)$$

in which ε is the molar absorbance in units of $mol^{-1}\,cm^{-1}\,L^{-1}$, the index sum runs over the number of computed excitation energies ω_i (expressed in cm^{-1}) with corresponding oscillator strengths f_i, and $\Delta_{1/2}$ is the half-weight bandwidth assumed to be constant and equal to 1200 cm^{-1}.

The atoms in molecules (AIM) theory and natural bond orbital (NBO) analysis were used to study some selected SubPz (B, Al, Ga) structures.[20,21] AIM is a useful tool based on the topological analysis of electron density. By obtaining the molecular graph of a given system, the strength and nature of bonding can be measured by looking at the values at the bond critical points (BCPs), which are first-order saddle points of the electron density. NBO analysis allows one to describe a system by a Lewis-like molecular bonding pattern, thus revealing localized two-electron bonds and lone pairs. Both tools help to give an accurate picture of the main differences in bonding of these boron, aluminum, and gallium SubPz molecules.

2. Results and Discussion

Optimized Structures and Geometrical Features

The energies of the optimized structures of SubPz and SubPc with aluminum and gallium as central metals are listed in Tables S1 and S2 in the Supporting Information. Two examples of SubPz and SubPc molecules are shown in Figure 1. For the sake of a better comparison with previous work on the boron-containing analogues, we used three different types of substituents: alkyl chains (R, H), thiol chains (–SR), and halogen atoms (F, Cl). The compounds included in our survey are labeled as SubPz (A, R) and SubPc (A, R), in which A is a fluorine or chlorine atom and R is H, F, CH_3, C_3H_7, SCH_3, SC_2H_5, and SPh.

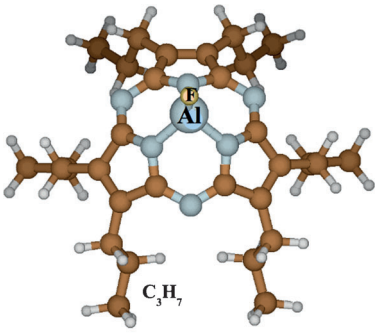

SubPz (M = Al, A = F, R = C_3H_7-*dd*)

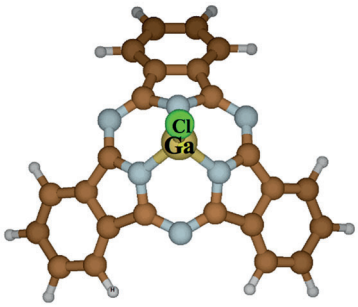

SubPc (M = Ga, A = Cl, R = H)

Figure 1. SubPz (A, R) (left) and SubPc (A, R) (right) pictures of two particular representative examples of the optimized structures at the B3LYP/6-31G(d) level.

For those derivatives in which the substituents are C_3H_7, SCH_3, and SC_2H_5, several conformers are possible depending on the relative orientations of the alkyl chains with respect to the molecular cone. Three different orientations were considered: up–up (uu), up–down (ud), and down–down (dd) (see Figure 1 for a dd example). The nomenclature "up" and "down" means that the chains are at different sides of the molecular cone: in the up conformation they are at the convex

side of the cone and in the down conformation they are at the concave side of the cone.

As expected, the optimized SubPz and SubPc are nonplanar molecules if aluminum and gallium are the central atoms of the cavity, the same behavior as that observed with boron.[14] Notably, these molecules do not always have a cone shape. For example, SubPc with carbon has been shown to be planar because of the ideal relationship between the covalent radius of the central atom and the cavity size.[10] The nonplanarity of our systems is an interesting property, because the concave and convex faces of the molecule can show a different behavior.[22] One remarkable feature of aluminum and gallium compounds with respect to those of boron is that the former have a much more closed cone shape. In SubPz, this trend is readily visualized through the value of the N–metal (M)–N angle (there are three equivalent angles) as shown in Figure S1. Although the N–M–N angles in boron compounds vary from 103.9 to 104.9°, aluminum compounds have values between 90.7 and 91.5° and gallium from 89.1 to 90.0°. Also, the metal–N distances measured on the SubPz and SubPc cavities present a considerable increase, as expected. Boron compound distances fall in a range of 1.498–1.502 Å. For aluminum the M–N distances are 1.829–1.836 Å, and for gallium 1.866–1.876 Å. Similar trends for both angles and distances are observed in aluminum and gallium SubPc substituted structures. These results are in agreement with previous results for SubPc (Al/Ga, H) structures.[7] Another remarkable aspect is that the deviation of the distance and angle values from their average value, as a function of the nature of the substituent, is small (even smaller than in the boron case), no matter whether Al or Ga is the central ion or what substituents are used. The three six-membered rings combining N, C, and the metal determine completely the main structural features of the compound.

The structural changes on going from boron to aluminum and gallium shown in Figure S1 can be better explained by analyzing the bonding in these species (see NBO and AIM in the Computational Details section). For this purpose we selected, as a suitable example, the B-, Al-, and Ga-containing SubPz (F, H) derivatives. Taking into account that the natural electron deficiency of the Group 13 elements is enhanced because they are bonding to an electronegative element (F in our examples), it is not surprising that the NBO analysis shows that the three nitrogen atoms are bonded to B, Al, and Ga through typical dative bonds. Indeed, the second-order perturbation energies between the nitrogen lone pairs and the empty p orbitals of the central atom are large and consistently the electron population of these orbitals in the corresponding SubPz (F, H) derivative is also significant, as shown in Table 1.

There are, however, some subtle differences on going from B to Al and to Ga. The first conspicuous fact is that the interaction of the N atoms with B is much stronger than that with Al and Ga, and accordingly the NBO analysis detects three covalent bonds with the composition shown in Table 1. Two factors are behind this enhanced interaction: 1) a much more effective overlap between the N lone pairs and the p orbitals in the case of the B atom, because of the similar size of the atoms involved; and 2) the higher electron acceptor capacity of first-row atoms with respect to the second- or third-row analogues. These two effects are also mirrored in the natural charges at the central atom, which increase significantly on going from B (+1.159) to Al (+1.979) and to Ga (+1.795). Notably, all indexes indicate that the interaction with Al is weaker than that observed for Ga. This is not unexpected, since Ga is more electronegative than Al, because of the small screening effect of the complete $3d^{10}$ subshell.

Table 1. Characteristics of the M–N (M = B, Al, Ga) interactions for SubPz (F, H) derivatives and the population [e^-] of the initially empty p orbitals.

M	M–N interaction	p orbital population
B	0.461 B ($sp^{2.82}$) + 0.8871 N ($sp^{1.65}$)[a]	0.396
Al	LP (N)→np 330[b]	0.215
Ga	LP (N)→np 515[b]	0.242

[a] Weight and characteristics of hybrid orbitals participating in the B–N bonding molecular orbital. [b] Second-order orbital interaction energies [kJ mol^{-1}] between the N lone pair (LP) and the empty p orbitals of metal M.

The picture obtained through the AIM analysis is completely coherent with the NBO description discussed above (see Figure 2). The three identical values of the electron density at the BCPs between the three nitrogen atoms and the central atom (B, Al, Ga) clearly show that the strength of the interaction decreases significantly on going from B to Al, since the electron density decreases by a factor of two and increases slightly on going from Al to Ga. Notably, the aforementioned electron density decrease is also due to the fact that the size of one of the atoms increases significantly on going from B to Al. Also, consistently the electron density at the M–F (M = B, Al, Ga) BCPs changes following the same trend found above for the M–N (M = B, Al, Ga) BCPs.

The decrease in the N–M–N bond angle on going form B to Al and Ga is a well-known effect that is behind, for instance, the higher inversion barriers in phosphines than in amines.[23] This is a direct consequence of the much smaller participation of the s orbitals in the P lone pair in phosphines relative to

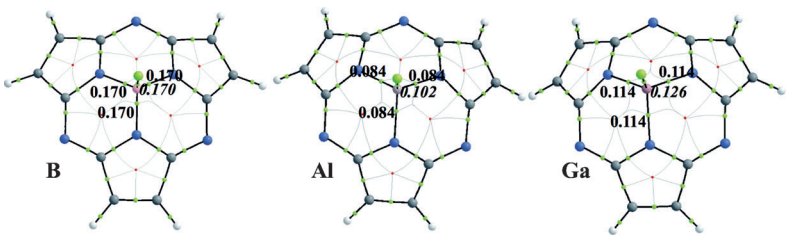

Figure 2. Molecular graphs of SubPz (F, H) with boron (left), aluminum (center), and gallium (right) from the AIM analysis. Bond critical points (BCPs) and ring critical points are green and red dots, respectively. BCP values from metal–N and metal–F bonds are highlighted with bold and italic characters, respectively.

amines. Accordingly, the bond angles centered at P are only slightly larger than 90°. The same effect occurs in the systems investigated if B is replaced by Al and Ga, which explains the angles shown in Figure S1.

The absolute electronic energies of the optimized structures SubPz (A, R) and SubPc (A, R) in the gas phase are collected in Tables S1 (Al) and S2 (Ga). Relative energies for the different orientations with the same substituent for each particular compound are also included, together with the results of the single-point B3LYP/6-31+G(d,p) calculations in chloroform. For those alkyl and thiol chains, three different orientations were considered: up–up (uu), up–down (ud), and down–down (dd), as described above. The results reveal that the uu, ud, and dd chains have an important effect on the stability of the structures. As expected, the uu conformers (those with the smaller steric repulsion) are the most stable ones in all cases, as occurred in the boron structures, although the difference between the conformers is larger here than in the boron case. This difference is especially remarkable in SubPz structures with thiol substituents. For a given conformer, the relative energy is not affected by the presence of F or Cl as A atom. Aluminum and gallium follow the same trends with respect to the substitution patterns.

Table 2. Q-band (λ_{max}) excitation energies in chloroform, oscillator strengths *f*, and dominant electronic transitions for aluminum-SubPz (A, R). $\Delta E_{H\text{-}L}$ is the energy gap between the HOMO and the LUMO [eV].

R	A	$\Delta E_{H\text{-}L}$	λ_{max} [eV]	λ_{max} [nm]	*f*	Main configuration[a]
H	F	3.18	2.85	435.7	0.188	H→L (91%), H−2→L(8%)
H	Cl	3.18	2.84	436.2	0.184	H→L (91%), H−2→L(8%)
CH_3	F	3.13	2.79	445.1	0.192	H→L (90%), H−2→L(8%)
F	F	3.25	2.89	428.5	0.138	H→L (87%), H−2→L(10%)
C_3H_7 (uu)	F	3.11	2.76	449.2	0.223	H→L (91%), H−2→L(7%)
C_3H_7 (ud)	F	3.10	2.75	451.5	0.201	H→L (91%), H−2→L(7%)
C_3H_7 (dd)	F	3.08	2.73	454.8	0.197	H→L (91%), H−2→L(7%)
C_3H_7 (uu)	Cl	3.11	2.76	449.8	0.217	H→L (91%), H−2→L(7%)
C_3H_7 (ud)	Cl	3.09	2.74	452.3	0.196	H→L (91%), H−2→L(7%)
C_3H_7 (dd)	Cl	3.07	2.72	455.4	0.192	H→L (91%), H−2→L(7%)
SCH_3 (uu)	F	2.78	2.67	464.8	0.445	H−2→L (68%), H→L(22%)
SCH_3 (ud)	F	2.76	2.37	522.8	0.178	H→L (86%), H−2→L (9%)
			2.87	432.0	0.296	H−2→L (74%), H→L (6%)
SCH_3 (uu)	Cl	2.77	2.66	466.1	0.440	H−2→L (72%), H→L (23%)
SCH_3 (ud)	Cl	2.76	2.37	523.8	0.173	H→L (89%), H−2→L (9%)
			2.86	433.8	0.299	H−2→L (75%)
SC_2H_5 (uu)	F	2.78	2.67	464.3	0.478	H−2→L (71%), H→L (23%)
SC_2H_5 (ud)	F	2.75	2.37	524.0	0.190	H→L (90%), H−2→L(8%)
			2.85	434.7	0.235	H−2→L (62%), H−3→L (12%), H−4→L (7%)
SC_2H_5 (dd)	F	2.87	2.56	483.9	0.074	H−1→L (63%), H→L (28%)
SC_2H_5 (uu)	Cl	2.78	2.66	465.7	0.474	H−2→L (66%), H→L (24%)
SC_2H_5 (ud)	Cl	2.75	2.36	524.9	0.185	H→L (90%), H−2→L (8%)
			2.84	435.9	0.249	H−2→L (64%), H−3→L (16%), H→L (6%)
SC_2H_5 (dd)	Cl	2.87	2.56	484.3	0.073	H−1→L (64%), H→L (28%)

[a] H and L stand for HOMO and LUMO, respectively.

Table 3. Q-band (λ_{max}) excitation energies in chloroform, oscillator strengths *f*, and dominant electronic transitions for aluminum-SubPc (A, R). $\Delta E_{H\text{-}L}$ is the energy gap between the HOMO and the LUMO [eV].

R	A	$\Delta E_{H\text{-}L}$	λ_{max} [eV]	λ_{max} [nm]	*f*	Main configuration[a]
H	F	2.63	2.34	530.4	0.375	H→L (97%)
H	Cl	2.62	2.33	531.7	0.368	H→L (97%)
CH_3	F	2.61	2.31	536.1	0.398	H→L (97%)
F	F	2.67	2.38	520.9	0.353	H→L (96%)
4F	Cl	2.57	2.29	541.9	0.379	H→L (97%)
4F	F	2.57	2.29	540.8	0.386	H→L (97%)
SCH_3	F	2.50	2.19	566.3	0.438	H→L (96%)
SPh (uu)	F	2.49	2.17	571.7	0.493	H→L (97%)

[a] H and L stand for HOMO and LUMO, respectively.

UV–Visible Spectra

In porphyrins, the Soret or B band consists of a strong transition to the second excited state at about 400 nm ($S_0 \rightarrow S_2$). The Q band consists of a weak transition to the first excited state at about 550 nm ($S_0 \rightarrow S_1$), which can be explained through the well-known four-orbital model of Gouterman. In this model, the photochemical activity is presumed to come from transitions involving the HOMO, HOMO−1, LUMO, and LUMO+1 orbitals, which would constitute the Q band. The rest of the absorptions of the spectra form the B band at lower wavelengths. This model is also commonly used to interpret the SubPz and SubPc spectra, which also have two main Q and B bands (450–650 and 300–350 nm, respectively) with similar characteristics to those observed in Pc. The values of λ_{max} and the oscillator strengths of the Q-band transitions for the different SubPz (A, R) and SubPc (A, R) molecules are collected in Tables 2 and 3 for Al-containing systems and Tables S3 and S4 for Ga-containing systems. These tables also show the main configuration of the frontier orbitals involved in the electronic transitions and the HOMO–LUMO energy gap.

As in the boron case, the HOMO−1 and LUMO orbitals of the aluminum and gallium SubPz (A, R) and SubPc (A, R) compounds are, in practically all cases, twofold degenerated. In the aluminum-SubPz case with R=H, alkyl (first rows in Table 2) the main contribution comes from the HOMO→LUMO transition (≈90%), whereas the remaining contributions (≈10%) come essentially from a (HOMO−2)→LUMO transition. The type of transition involved, as can be deduced from Figure 3, is mainly a π–π* excitation. In the boron case no transitions involving either LUMO+1 or HOMO−1 had been observed, and aluminum and gallium share this feature.

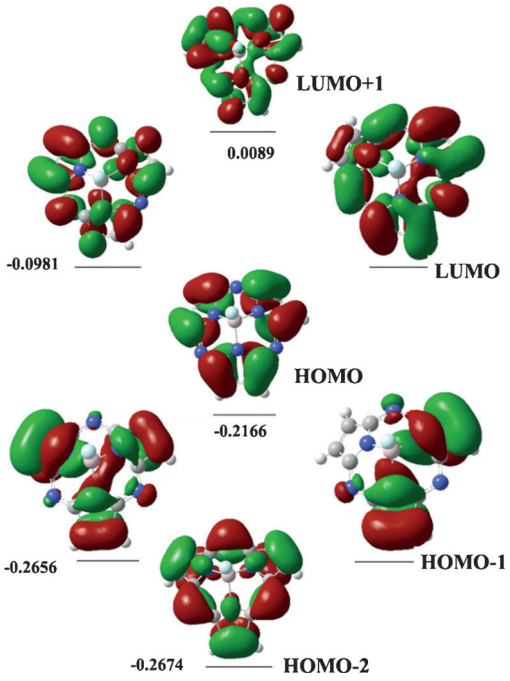

Figure 3. Frontier orbitals of aluminum-SubPz (F, H) and energy values [hartrees].

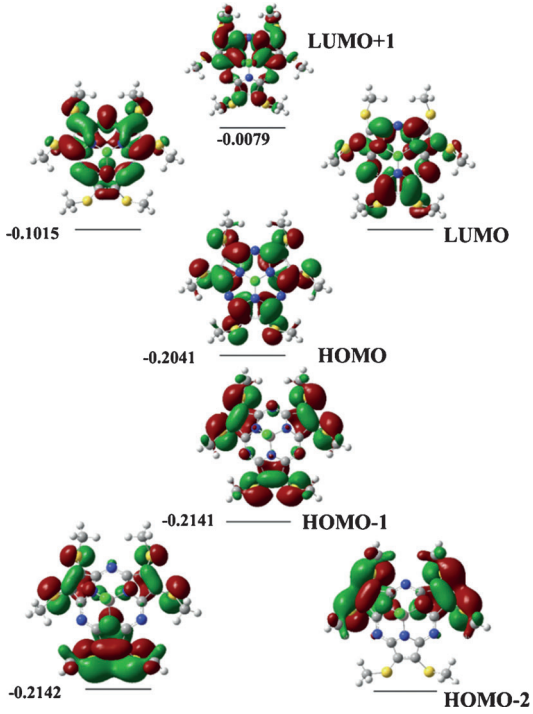

Figure 4. Frontier orbitals of aluminum-SubPz (Cl, SCH_3) and energy values [hartrees].

For aluminum-SubPz with R = SCH_3, SC_2H_5 (Table 2) there is a more complex panorama because of the presence of two Q-band peaks in the region 400–550 nm. The most intense one is located in lower wavelengths at about 2.87 eV (432 nm), in the case of the ud conformer (F, SCH_3), with an oscillator strength about 0.297, whereas the less intense transition is sited at approximately 2.37 eV (522 nm) for the same conformer with a smaller value of *f* (about 0.178). This latter entity depends on the thiol group orientation. In fact, if the substituents are oriented uu, the estimated oscillator strength for the higher-wavelength transition is negligible (the reason why it has been omitted in Table 2). Concerning the frontier molecular orbitals involved in both transitions, it can be observed that at the highest wavelengths the HOMO→LUMO transition has the major contribution (about 89%) and it corresponds to a $\pi \rightarrow \pi^*$ electronic transition (see Figure 4). Remarkably, in the most intense Q band the transition is mainly $n \rightarrow \pi^*$. The Q band observed at 2.86 eV (433.8 nm) in the case of (Cl, SCH_3) has 75% participation of the (HOMO−2)→LUMO transition, in agreement with the boron case. This is not true on dealing with the conformer dd of (Cl, SC_2H_5), for which the main contribution to lower Q band appears to be provided by a (HOMO−1)→LUMO transition. Indeed, if one observes the energy gap between the HOMO−1 and HOMO−2, it presents a small value (about 0.04 eV) in all the thiol conformers and consequently is quasi-degenerated. Moreover, the similitude of electronic density distribution in these molecular orbitals seems to indicate that the lower Q band is an $n \rightarrow \pi^*$ transition no matter whether the HOMO−1 and HOMO−2 are involved in the transition. For gallium (Table S3) the same general characteristics described for aluminum were observed.

Although all the data for each spectrum are not tabulated for the sake of conciseness, the spectra of SubPz (A, R) with R = H, F, CH_3, and C_3H_7 substituents can be roughly described by two intense peaks in the B-band region and one main peak, of lower intensity, in the Q-band region. SubPz (A, R) structures with R = SCH_3 or SC_2H_5 have a poorer B band with smaller peaks than the alkyl-substituted ones. For the most stable conformers (SCH_3 (uu), SC_2H_5 (uu)) there are, as has been mentioned above, two peaks in the Q region which, in contrast to the alkyl derivatives, are the most intense of the whole spectrum.

Let us now analyze and compare some particular cases. Figure 5 provides an overview of the spectral evolution of SubPz (F, CH_3) on going from boron to gallium. All three metals share the same profile, and even though there are some small differences in the B band, Al and Ga have almost exactly the same Q band. The aluminum spectrum is redshifted with respect to that of boron by almost 12 nm (see Figure 5). There is an extension of the π conjugation on passing from boron to aluminum and gallium, a feature that can also be appreciated from the energy gap of 3.13 eV (2.86 eV with boron).

Figure 6 shows the effect of the substitution pattern in the aluminum-SubPz (Cl, C_3H_7) structures. All three conformers, uu (the most stable one), ud, and dd, present the same behavior and it is not possible to distinguish them from the spectra. This situation does not change upon changing either the nature of the A atom (F or Cl) or that of the central metal (B, Al, Ga).

The most interesting case for the substitution patterns is that of the thiol derivatives with R = SCH_3, SC_2H_5. Figure 7 illustrates the particular case of aluminum-SubPz (Cl, SC_2H_5) con-

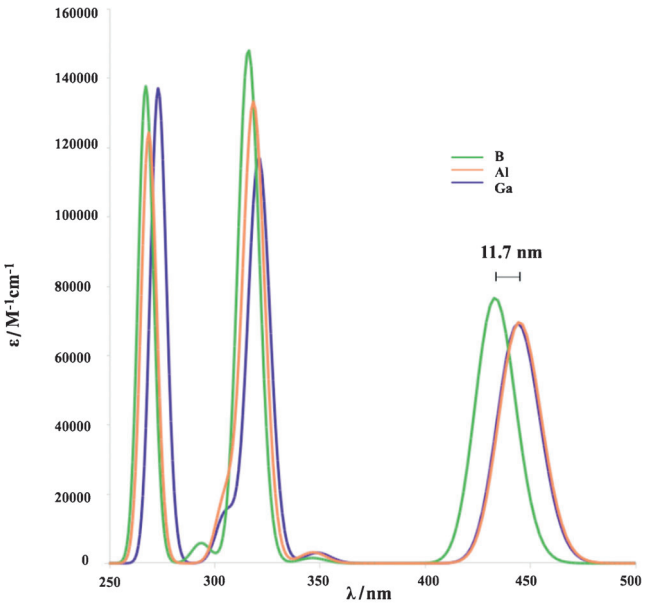

Figure 5. Simulated TDDFT UV/Vis spectra of SubPz (F, CH_3) with M = B, Al, Ga in chloroform at the B3LYP/6-31 + G(d,p) level.

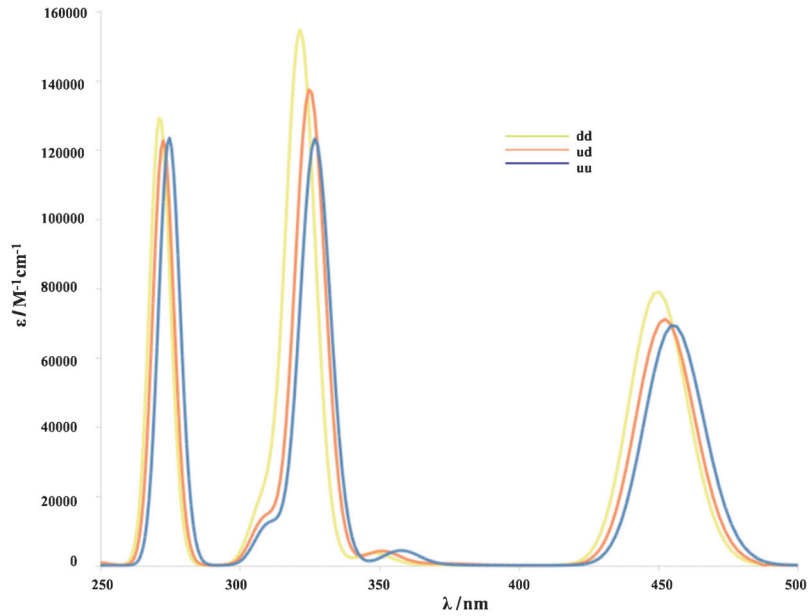

Figure 6. Simulated TDDFT UV/Vis spectra of the different conformers of SubPz (Cl, C_3H_7) with M = Al in chloroform at the B3LYP/6-31 + G(d,p) level.

formers, as suitable examples. The energy difference between uu and dd conformers is large (see Table S1), so the latter is predicted to be in such a minority that its presence does not affect the shape of the spectra. However, in this case it would be possible to distinguish the three conformers from their spectra, as the shape and position of the bands are quite different. On the one hand, the dd conformer has a unique peak in the B band and a quite broad absorption band that goes from 400 nm to approximately 570 nm, which results from a mixture of absorptions of low intensity. The most stable uu conformer has no significant absorptions in the B-band region, but shows an intense peak in the Q region at 465.7 nm, about 10 nm blueshifted with respect to that of boron (476.1 nm) and almost identical to that of gallium (465.4 nm). Finally, the ud conformer presents two well-defined Q bands centered at 425 and 530 nm, and two less intense bands in the B region.

The evolution of the spectra of the SubPc (A, R) compounds on changing the metal from boron to gallium is shown in Figure 8. SubPc (A, R) have simpler spectra, with an intense peak in the Q region that is about 15 nm redshifted on going from boron to aluminum and gallium, and a similarly strong band in the B region centered at about 340 nm, which is always accompanied by a much weaker one at about 320 nm and another very weak one at about 280 nm. Note also the significant overlap of the absorption bands of Al and Ga, in particular as far as the Q bands are concerned. There are, however, significant differences if the spectrum of the SubPc (F, CH_3) species is compared with that of the SubPz (F, CH_3) analogues (Figure 5). These dissimilarities are particularly apparent for the B bands. The very weak band observed for the SubPc (F, CH_3) species at around 280 nm becomes a very strong one. The second one at around 320 nm is a 20 nm redshifted shoulder and the strong absorption at 340 nm appears also about 20 nm redshifted in the SubPz (F, CH_3) compounds. There are also non-negligible differences as far as the position and the relative intensity of the Q band (see Table 3) are concerned. In the SubPc (F, CH_3) derivatives the Q band appears significantly blueshifted (by about 90 nm) with respect to those in SubPz (F, CH_3), whereas their relative intensity with respect to the B bands also increases significantly.

3. Conclusions

Our DFT theoretical survey of aluminum- and gallium-containing SubPz and SubPc molecules shows some geometrical differences with respect to their boron-containing analogues, especially a more acute cone shape. These geometrical changes reflect the different hybridization patterns on going from a first-row atom to the second- and third-row analogues. The relative disposition of the alkyl chain and thiol chain substituents has an important effect on the relative energy of these conformers, which is larger than in the boron analogues. This effect is particularly dramatic in the characteristics of the UV/Vis spectra of the SC_2H_5-substituted derivatives. The HOMO−1 and LUMO or-

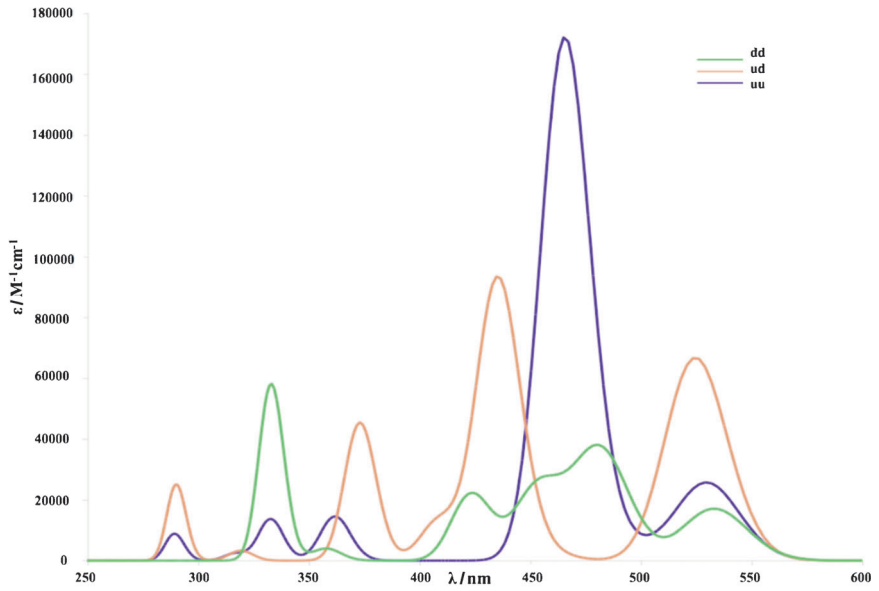

Figure 7. Simulated TDDFT UV/Vis spectra of the different conformers of SubPz (Cl, SC_2H_5) with M = Al in chloroform at the B3LYP/6-31 + G(d,p) level.

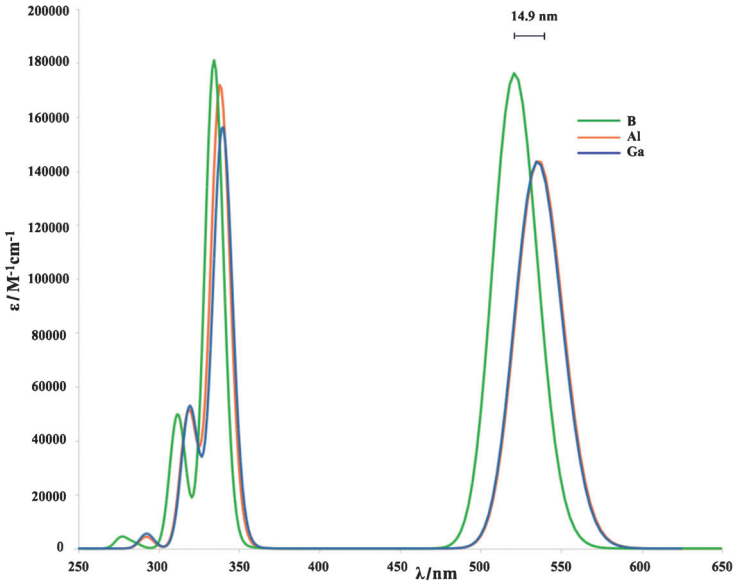

Figure 8. Simulated TDDFT UV/Vis spectra of the different conformers of SubPc (F, CH_3) with M = B, Al, Ga in chloroform at the B3LYP/6-31 + G(d,p) level.

bitals are twofold degenerated for both SubPz and SubPc systems, as occurred in the corresponding boron compounds. The replacement of boron by aluminum or gallium leads to small changes in both the relative intensities of the bands and their relative position. In fact, the absorption bands of SubPz (Al, Ga) are redshifted with respect to those of the SubPz (B) if R = H, alkyl, but blueshifted if R = SCH_3, SC_2H_5. Conversely, the absorptions of SubPc (Al, Ga) structures are redshifted and with smaller energy gaps with respect to SubPc (B) for all kinds of R substituents. Nevertheless, the HOMO→LUMO transitions are the dominant ones in most cases, but (HOMO−2)→LUMO transitions are especially important in the thiol-substituted structures. The similarities between aluminum and gallium spectra seem to indicate that the presence of a complete 3d subshell in the gallium atom does not play any significant role. From the characteristics of their absorption spectra, one may conclude that the aluminum- and gallium-containing derivatives investigated may also have, as their boron-containing analogues, promising photochemical properties.

Acknowledgements

This work was partially supported by the DGI Project No. CTQ2009-13129, by the Project MADRISOLAR2, Ref.: S2009PPQ/1533, of the Comunidad Autónoma de Madrid, and by Consolider on Molecular Nanoscience CSC2007-00010. A generous allocation of computing time at the CCC of the UAM is also acknowledged.

Keywords: density functional calculations · subphthalocyanines · subporphyrazines · substituent effects · UV/Vis spectroscopy

[1] M. Grätzel, *Inorg. Chem.* **2005**, *44*, 6841 – 6851.
[2] H. B. Gray, *Nat. Chem.* **2009**, *1*, 7.
[3] V. I. Vullev, *J. Phys. Chem. Lett.* **2011**, *2*, 503 – 508.
[4] L. R. Milgrom, *The Colours of Life: An Introduction to the Chemistry of Porphyrins and Related Compounds*, Springer, Berlin, **1997**.
[5] a) T. Torres, *Angew. Chem.* **2006**, *118*, 2900 – 2903; *Angew. Chem. Int. Ed.* **2006**, *45*, 2834 – 2837; b) C. G. Claessens, D. González-Rodríguez, T. Torres, *Chem. Rev.* **2002**, *102*, 835 – 853.
[6] A. Zafirov, S. Rakovski, J. Bakardjieva-Eneva, L. Prahov, L. Assenova, F. Marrandino, PCT Int. Appl. WO-2002080158, **2002**.
[7] Y. Yang, *Polyhedron* **2012**, *33*, 310 – 318.
[8] E. J. Baerends, G. Ricciardi, A. Rosa, S. J. A. van Gisbergen, *Coord. Chem. Rev.* **2002**, *230*, 5 – 27.
[9] A. Rosa, G. Ricciardi, *J. Phys. Chem. A* **2001**, *105*, 3311 – 3327.
[10] D. Zdravkovski, M. C. Milletti, *J. Mol. Struct. THEOCHEM* **2005**, *717*, 85 – 89.
[11] J. Yang, Z. M. Su, *Int. J. Quantum Chem.* **2005**, *103*, 54 – 59.
[12] F. Pichierri, *Chem. Phys. Lett.* **2006**, *426*, 410 – 414.
[13] A. Medina, C. G. Claessens, G. M. A. Rahman, A.-M. Lamsabhi, O. Mó, M. Yáñez, D. M. Guldi, T. Torres, *Chem. Commun.* **2008**, 1759 – 1761.
[14] A.-M. Lamsabhi, M. Yáñez, O. Mó, C. Trujillo, F. Blanco, I. Alkorta, J. Elguero, E. Caballero, M. S. Rodríguez-Mogarde, C. G. Claessens, T. Torres, *J. Porphyrins Phthalocyanines* **2011**, *15*, 1220 – 1230.
[15] Gaussian 09 (Revision B.01), M. J. Frisch, G. W. Trucks, H. B. Schlegel, G. E. Scuseria, M. A. Robb, J. R. Cheeseman, G. Scalmani, V. Barone, B. Mennucci, G. A. Petersson, H. Nakatsuji, M. Caricato, X. Li, H. P. Hratchian, A. F. Izmaylov, J. Bloino, G. Zheng, J. L. Sonnenberg, M. Hada, M. Ehara,

K. Toyota, R. Fukuda, J. Hasegawa, M. Ishida, T. Nakajima, Y. Honda, O. Kitao, H. Nakai, T. Vreven, J. A. Montgomery, Jr., J. E. Peralta, F. Ogliaro, M. Bearpark, J. J. Heyd, E. Brothers, K. N. Kudin, V. N. Staroverov, R. Kobayashi, J. Normand, K. Raghavachari, A. Rendell, J. C. Burant, S. S. Iyengar, J. Tomasi, M. Cossi, N. Rega, J. M. Millam, M. Klene, J. E. Knox, J. B. Cross, V. Bakken, C. Adamo, J. Jaramillo, R. Gomperts, R. E. Stratmann, O. Yazyev, A. J. Austin, R. Cammi, C. Pomelli, J. W. Ochterski, R. L. Martin, K. Morokuma, V. G. Zakrzewski, G. A. Voth, P. Salvador, J. J. Dannenberg, S. Dapprich, A. D. Daniels, Ö. Farkas, J. B. Foresman, J. V. Ortiz, J. Cioslowski, D. J. Fox, Gaussian, Inc., Wallingford CT, **2009**.

[16] a) A. D. Becke, *J. Chem. Phys.* **1993**, *98*, 5648 – 5652; b) C. Lee, W. Yang, R. G. Parr, *Phys. Rev. B* **1988**, *37*, 785 – 789.

[17] a) R. Bauernschmitt, R. Ahlrichs, *Chem. Phys. Lett.* **1996**, *256*, 454 – 464; b) A. Dreuw, M. Head-Gordon, *Chem. Rev.* **2005**, *105*, 4009 – 4037.

[18] J. Tomasi, B. Mennuci, R. Cammi, *Chem. Rev.* **2005**, *105*, 2999 – 3094.

[19] a) S. I. Gorelsky, *SWizard program*, http://www.sg-chem.net/, University of Ottawa, Ottawa, Canada, **2010**; b) S. I. Gorelsky, A. B. P. Lever, *J. Organomet. Chem.* **2001**, *635*, 187 – 196.

[20] a) R. F. W. Bader, *Atoms in Molecules: A Quantum Theory*, Clarendon, Oxford, **1990**; b) A. D. Becke, K. E. Edgecombe, *J. Chem. Phys.* **1990**, *92*, 5397 – 5403.

[21] a) J. P. Foster, F. Weinhold, *J. Am. Chem. Soc.* **1980**, *102*, 7211 – 7218; b) A. E. Reed, F. Weinhold, *J. Chem. Phys.* **1983**, *78*, 4066 – 4073; c) A. E. Reed, R. B. Weinstock, F. Weinhold, *J. Chem. Phys.* **1985**, *83*, 735 – 746.

[22] D. González-Rodríguez, T. Torres, D. M. Guldi, J. Rivera, M. A. Herranz, L. Echegoyen, *J. Am. Chem. Soc.* **2004**, *126*, 6301 – 6313.

[23] J. M. Lehn, B. Munsch, *J. Chem. Soc. D* **1969**, 1327 – 1329.

Received: December 10, 2012
Published online on February 21, 2013